

## Effective Dissipation and Turbulence in Spectrally Truncated Euler Flows

Cyril Cichowlas,<sup>1</sup> Pauline Bonaïti,<sup>1</sup> Fabrice Debbasch,<sup>2</sup> and Marc Brachet<sup>1</sup>

<sup>1</sup>Laboratoire de Physique Statistique de l'École Normale Supérieure, associé au CNRS et aux Universités, Paris VI et VII, 24 Rue Lhomond, 75231 Paris, France

<sup>2</sup>ERGA, CNRS UMR 8112, 4 Place Jussieu, F-75231 Paris Cedex 05, France

(Received 21 October 2004; published 22 December 2005)

A new transient regime in the relaxation towards absolute equilibrium of the conservative and time-reversible 3D Euler equation with a high-wave-number spectral truncation is characterized. Large-scale dissipative effects, caused by the thermalized modes that spontaneously appear between a transition wave number and the maximum wave number, are calculated using fluctuation dissipation relations. The large-scale dynamics is found to be similar to that of high-Reynolds number Navier-Stokes equations and thus obeys (at least approximately) Kolmogorov scaling.

DOI: 10.1103/PhysRevLett.95.264502

PACS numbers: 47.27.Eq, 05.20.Jj, 83.60.Df

Turbulence has been observed in inviscid and conservative systems, in the context of (compressible) low-temperature superfluid turbulence [1–3]. This behavior has also been reproduced using simple (incompressible) Biot-Savart vortex methods, which amount to Eulerian dynamics with *ad hoc* vortex reconnection [4]. The purpose of this Letter is to study the dynamics of spectrally truncated 3D incompressible Euler flows. Our main result is that the inviscid and conservative Euler equation, with a high-wave number spectral truncation, has long-lasting transients that behave just as those of the dissipative (with generalized dissipation) Navier-Stokes equation. This is so because the thermalized modes between some transition wave number and the maximum wave number can act as a fictitious microworld providing an effective viscosity to the modes with wave numbers below the transition wave number.

We thus study general solutions to the finite system of ordinary differential equations for the complex variables  $\hat{\mathbf{v}}(\mathbf{k})$  [ $\mathbf{k}$  is a 3D vector of relative integers ( $k_1, k_2, k_3$ ) satisfying  $\sup_\alpha |k_\alpha| \leq k_{\max}$ ]

$$\partial_t \hat{v}_\alpha(\mathbf{k}, t) = -\frac{i}{2} \mathcal{P}_{\alpha\beta\gamma}(\mathbf{k}) \sum_{\mathbf{p}} \hat{v}_\beta(\mathbf{p}, t) \hat{v}_\gamma(\mathbf{k} - \mathbf{p}, t), \quad (1)$$

where  $\mathcal{P}_{\alpha\beta\gamma} = k_\beta P_{\alpha\gamma} + k_\gamma P_{\alpha\beta}$  with  $P_{\alpha\beta} = \delta_{\alpha\beta} - k_\alpha k_\beta / k^2$  and the convolution in (1) is truncated to  $\sup_\alpha |k_\alpha| \leq k_{\max}$ ,  $\sup_\alpha |p_\alpha| \leq k_{\max}$ , and  $\sup_\alpha |k_\alpha - p_\alpha| \leq k_{\max}$ .

This system is time reversible and exactly conserves the kinetic energy  $E = \sum_k E(k, t)$ , where the energy spectrum  $E(k, t)$  is defined by averaging  $\mathbf{v}$  on spherical shells of width  $\Delta k = 1$ ,

$$E(k, t) = \frac{1}{2} \sum_{k-\Delta k/2 < |\mathbf{k}'| < k+\Delta k/2} |\hat{\mathbf{v}}(\mathbf{k}', t)|^2. \quad (2)$$

The discrete Eq. (1) is classically obtained [5] by performing a Galerkin truncation [ $\hat{\mathbf{v}}(\mathbf{k}) = 0$  for  $\sup_\alpha |k_\alpha| \leq k_{\max}$ ] on the Fourier transform  $\mathbf{v}(\mathbf{x}, t) = \sum \hat{\mathbf{v}}(\mathbf{k}, t) e^{i\mathbf{k}\cdot\mathbf{x}}$  of a spatially periodic velocity field obeying the (unit density)

three-dimensional incompressible Euler equations,

$$\partial_t \mathbf{v} + (\mathbf{v} \cdot \nabla) \mathbf{v} = -\nabla p, \quad \nabla \cdot \mathbf{v} = 0. \quad (3)$$

The short-time, spectrally converged truncated Eulerian dynamics (1) has been studied [6,7] to obtain numerical evidence for or against blowup of the original (untruncated) Euler Eq. (3). We study here the behavior of solutions of (1) when spectral convergence to solutions of (3) is lost. Long-time truncated Eulerian dynamics is relevant to the limitations of standard simulations of high-Reynolds number (small viscosity) turbulence that are performed using Galerkin truncations of the Navier-Stokes equation [8].

Equation (1) is solved numerically using standard [9] pseudospectral methods with resolution  $N$ . The solutions are dealiased by spectrally truncating the modes for which at least one wave-vector component exceeds  $N/3$  (thus a  $1600^3$  run is truncated at  $k_{\max} = 534$ ). This method allows the exact evaluation of the Galerkin convolution in (1) in only  $N^3 \log N$  operations. Time marching is done with a second-order leapfrog finite-difference scheme, even and odd time steps are periodically recoupled using fourth-order Runge-Kutta.

To study the dynamics of (1), we use the so-called Taylor-Green [10] single-mode initial condition of (3)  $u^{\text{TG}} = \sin x \cos y \cos z$ ,  $v^{\text{TG}} = -u^{\text{TG}}(y, -x, z)$ ,  $w^{\text{TG}} = 0$ . Symmetries are employed in a standard way [11] to reduce memory storage and speed up computations. Runs were made with  $N = 256, 512, 1024$ , and  $1600$ .

Figure 1 displays the time evolution (top) and resolution dependence (bottom) of the energy spectra. Each energy spectrum  $E(k, t)$  admits a minimum at  $k = k_{\text{th}}(t) < k_{\max}$ , in sharp contrast with the short-time ( $t \leq 4$ ) spectrally converged Eulerian dynamics (data not shown, see [7,11]). For  $k > k_{\text{th}}(t)$  the energy spectrum obeys the scaling law  $E(k, t) = c(t)k^2$  (see the dashed line at the bottom of the figure). The dynamics thus spontaneously generates a scale separation at wave number  $k_{\text{th}}(t)$ . Figure 1 also shows that  $k_{\text{th}}$  slowly decreases with time. For fixed  $k$  inside the  $k^2$

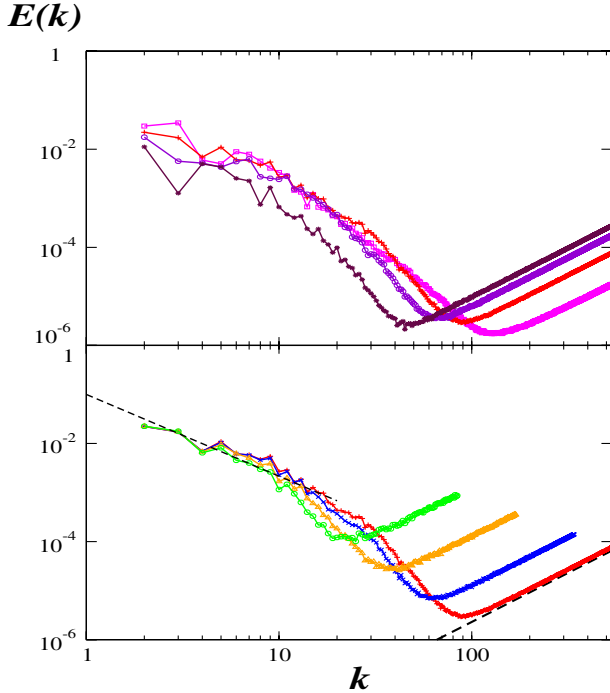


FIG. 1 (color online). Energy spectra. Top: resolution  $1600^3$  at  $t = (6.5, 8, 10, 14)$  ( $\diamond, +, \circ, *$ ); bottom: resolutions  $256^3$  (circle  $\circ$ ),  $512^3$  (triangle  $\Delta$ ),  $1024^3$  (cross  $\times$ ), and  $1600^3$  (cross  $+$ ) at  $t = 8$ . The dashed lines indicate  $k^{-5/3}$  and  $k^2$  scalings.

scaling zone  $E(k, t)$  increases with time but  $E(k, t)$  decreases with time for  $k$  close (but inferior) to  $k_{th}(t)$ .

The traditionally expected [5,12] asymptotic dynamics of the system is to reach an absolute equilibrium, which is a statistically stationary exact solution of the truncated Euler equations, with energy spectrum  $E(k) = ck^2$ . Our new results (see Fig. 1) show that a time-dependent statistical equilibrium appears long before the system reaches its stationary state. Indeed, the early appearance of a  $k^2$  zone is the key factor in the relaxation of the system towards the absolute equilibrium: as time increases, more and more modes gather into a time-dependent statistical equilibrium, which itself tends towards an absolute equilibrium.

Since the total energy  $E$  is constant, the energy dissipated from large scales into the time-dependent statistical equilibrium is given by

$$E_{th}(t) = \sum_{k_{th}(t) < k} E(k, t). \quad (4)$$

The time evolutions of  $k_{th}$  and  $E_{th}$  are presented in Fig. 2. The figure clearly displays the long transient during which, for all resolutions,  $k_{th}$  decreases and  $E_{th}$  increases with time. Note that, at all times,  $k_{th}$  increases and  $E_{th}$  decreases with the resolution.

Since the energy of the time-dependent equilibrium increases with time, the modes outside the equilibrium

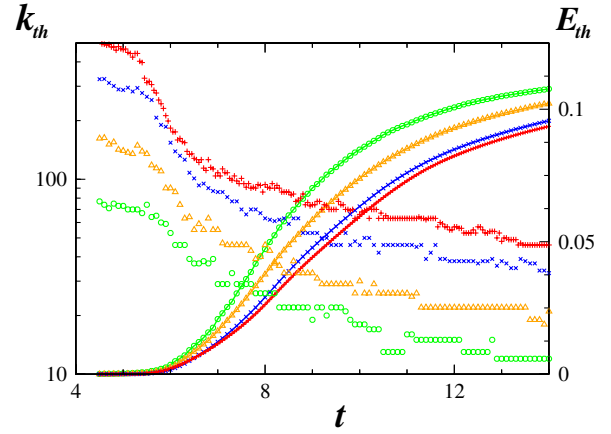


FIG. 2 (color online). Time evolution of  $k_{th}$  (left vertical axis) and  $E_{th}$  (right vertical axis) at resolutions  $256^3$  (circle  $\circ$ ),  $512^3$  (triangle  $\Delta$ ),  $1024^3$  (cross  $\times$ ), and  $1600^3$  (cross  $+$ ).

lose energy. The presence of a time-dependent equilibrium thus induces an effective dissipation on the lower  $k$  modes.

We now estimate the characteristic time of effective dissipation  $\tau(k_d)$  of modes  $k_d$  close to  $k_{th}(t)$  by assuming time-scale separation and studying, at each time  $t$ , the relaxation towards the *time-independent* absolute equilibrium characterized by  $E_{th}(t)$  and  $k_{max}$ . The existence of a fluctuation dissipation theorem (FDT) [13,14] ensures that dissipation around the equilibrium has the same characteristic time scale as the equilibrium correlation functions  $\langle \hat{v}_\alpha(\mathbf{k}, t) \hat{v}_\beta(\mathbf{k}', 0) \rangle$  [brackets denote equilibrium statistical averaging over initial conditions  $\hat{v}_\beta(\mathbf{k}', 0)$ ]. Defining this time scale  $\tau_C$  as the parabolic decorrelation time

$$\tau_C^2 \partial_{tt} \langle \hat{v}_\alpha(\mathbf{k}, t) \hat{v}_\beta(\mathbf{k}', 0) \rangle|_{t=0} = \langle \hat{v}_\alpha(\mathbf{k}, 0) \hat{v}_\beta(\mathbf{k}', 0) \rangle, \quad (5)$$

time translation invariance allows one to express the second-order time derivative as  $-\langle \partial_t \hat{v}_\alpha(\mathbf{k}, t) \times \partial_{t'} \hat{v}_\beta(\mathbf{k}', t') \rangle|_{t=t'=0}$ . Using expression (1) for the time derivatives reduces the evaluation of  $\tau_C$  to that of an equal-time fourth-order moment of a Gaussian field with correlation  $\langle \hat{v}_\alpha(\mathbf{k}, t) \hat{v}_\beta(-\mathbf{k}, t) \rangle = AP_{\alpha\beta}(\mathbf{k})$  [5] where  $A = E_{th}/(2k_{max})^3$ . The only nonvanishing contribution is a one loop graph [8,15]. The correlation time  $\tau_C$  associated with wave number  $k$  is found in this way [14] to obey the simple scaling law

$$\tau_C = \frac{C}{k\sqrt{E_{th}}}, \quad (6)$$

where  $C = 1.43382$  is a constant of order unity. The time scale  $\tau_C$  is the eddy turnover time at wave number  $k_{th}$ . Because of Kolmogorov (K41) behavior (see below) the evolution of  $E_{th}$  is governed by the large-eddy turnover time. The assumption of time-scale separation made above is thus consistent.

This strongly suggests the introduction of an effective generalized Navier-Stokes model for the dissipative dy-

namics of modes  $k$  close to  $k_{\text{th}}(t)$ . To wit, we make the ansatz  $\varepsilon(k, t) = \bar{\nu}|k|E(k, t)$ , where  $\bar{\nu} = \sqrt{E_{\text{th}}}/C$  and  $\varepsilon(k, t) = -\partial E(k, t)/\partial t$  is the spectral density of energy dissipation

$$\varepsilon(t) = \frac{dE_{\text{th}}(t)}{dt}. \quad (7)$$

Assuming that this dissipation takes place in a range of width  $\alpha k_d$  around  $k_d$ , we estimate the total dissipation  $\varepsilon \sim \bar{\nu} k_d E(k_d) \alpha k_d$ . This, together with  $E(k_d) \sim k_d^2 E_{\text{th}}/k_{\text{max}}^3$  yields the relation

$$k_d \sim \left( \frac{\varepsilon}{E_{\text{th}}^{3/2}} \right)^{1/4} k_{\text{max}}^{3/4}. \quad (8)$$

The consistency of this estimation of effective dissipation with the results displayed in Fig. 2 requires that  $k_d \sim k_{\text{th}}$ . The ratio  $k_{\text{th}}/k_d$  is displayed in Fig. 3. It is seen to be of order unity and is reasonably constant in time and resolution independent (at least for  $N > 256$ ).

Thus the small-scale modes between  $k_{\text{th}}$  and  $k_{\text{max}}$  act as a fictitious thermostat providing, via the FDT, an effective viscosity to the large-scale modes with wave numbers below  $k_{\text{th}}$ . Note that spontaneous equilibration happening in conservative isolated systems, such as the one studied in this Letter, should not be confused with equilibration resulting from interaction with the thermalized degrees of freedom of the molecules constituting a physical fluid. Indeed, the reversible dynamics of the isolated system (1) spontaneously generates both the wave number at which the fictitious thermostat begins and its temperature.

The previous results indicate scale separation between conservative large-scale and dissipative small-scale dynamics. Furthermore, the scale separation increases with

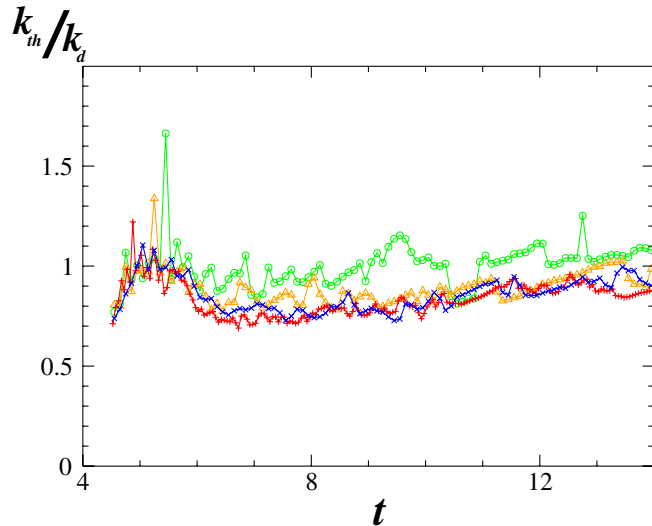


FIG. 3 (color online). Time evolution of the ratio  $k_{\text{th}}/k_d$  at resolutions  $256^3$  (circle  $\circ$ ),  $512^3$  (triangle  $\Delta$ ),  $1024^3$  (cross  $\times$ ), and  $1600^3$  (cross  $+$ ).

resolution. This strongly suggests that large-scale behavior may be identical to that of high-Reynolds number standard Navier-Stokes equations, which is known [8] to obey (at least approximately) K41 scaling.

The energy dissipation rate (7) shown on Fig. 4 (top, left axis) is in good agreement with the corresponding data for the Navier-Stokes Taylor-Green flow (see Ref. [11], Fig. 7, and Ref. [8], Fig. 5.12). Both the time for maximum energy dissipation  $t_{\text{max}} \approx 8$  and the value of the dissipation rate at that time  $\varepsilon(t_{\text{max}}) \approx 1.5 \times 10^{-2}$  are in quantitative agreement. Furthermore, the long-time quasilinear behavior of  $\varepsilon^{-1/3}$  (shown on the right axis) is compatible with K41 self-similar decay  $\varepsilon(t) \sim L_0^2 t^{-3}$ .

A confirmation for K41 behavior around  $t_{\text{max}}$  is displayed in Fig. 4 (bottom). The value of the inertial-range exponent  $n$ , obtained by low- $k$  least squares fits of the logarithm of the energy spectrum to the function  $c - n \log(k)$ , is close to  $5/3$  (horizontal dashed line) when  $t \approx t_{\text{max}}$ . The  $-5/3$  exponent is also shown as the left dashed line on the bottom of Fig. 1, where the dissipative effects can be traced back to the energy spectrum decreasing faster than  $k^{-5/3}$  at intermediate wave numbers.

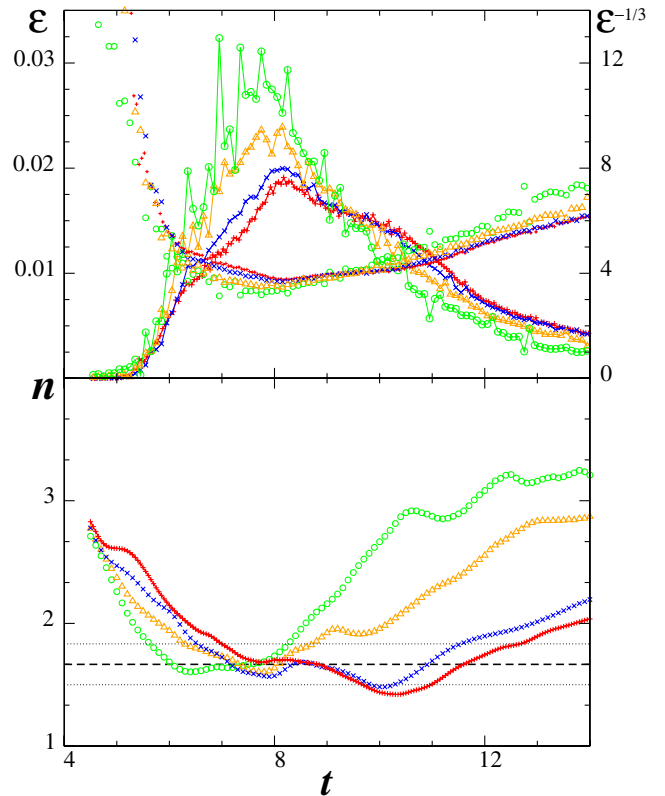


FIG. 4 (color online). Temporal evolution. Top: energy dissipation  $\varepsilon$  (left vertical axis) and  $\varepsilon^{-1/3}$  (right vertical axis); bottom:  $k^{-n}$  inertial-range exponent  $n$  at resolutions  $256^3$  (fit interval  $2 \leq k \leq 12$ , circle  $\circ$ ),  $512^3$  (fit interval  $2 \leq k \leq 14$ , triangle  $\Delta$ ),  $1024^3$  (fit interval  $2 \leq k \leq 16$ , cross  $\times$ ), and  $1600^3$  (fit interval  $2 \leq k \leq 20$ , cross  $+$ ).

The mixed K41-absolute equilibrium spectra have already been discussed in the wave turbulence literature (e.g., [16]) and have more recently been studied in connection with the Leith model of hydrodynamic turbulence [17]. In this context, small-scale thermalization may have some bearing on the so-called bottleneck problem if the dissipation wave number approaches  $k_{\max}$ .

Note that the dynamics of spectrally truncated time-reversible nonlinear equations has also been investigated in the special cases of 1D Burgers-Hopf models [18] and 2D quasigeostrophic flows [19]. A central point in these studies was the nature of the statistical equilibrium that is achieved at large times. Several equilibria are *a priori* possible because both (truncated) 1D Burgers-Hopf and 2D quasigeostrophic flow models admit, besides the energy, a number of additional conserved quantities. The 3D Euler case is of a different nature because (except for helicity that identically vanishes for the flows considered here) there is no known additional conserved quantity [8] and the equilibrium is thus unique. The central problem in truncated 3D Eulerian dynamics is therefore the mechanism of relaxation towards equilibrium, as studied in this Letter.

In summary, our main result is that the spectrally truncated Euler equation has long-lasting transients behaving just like those of the dissipative Navier-Stokes equation. The small-scale thermalized modes act as a fictitious micro-world providing an effective viscosity to the large-scale modes. These dissipative effects were estimated using a new exact result based on fluctuation dissipation relations. Furthermore, the solutions of the truncated Euler equations were shown to obey, at least approximately, K41 scaling. In this context, the spectrally truncated Euler equations appear as a minimal model of turbulence.

We acknowledge discussions with D. Bonn, U. Frisch, and Y. Pomeau. The computations were carried out on the NEC-SX5 computer of the Institut du Développement et des Ressources en Informatique Scientifique (IDRIS) of

the Centre National pour la Recherche Scientifique (CNRS).

- 
- [1] C. Nore, M. Abid, and M. E. Brachet, Phys. Rev. Lett. **78**, 3896 (1997).
  - [2] C. Nore, M. Abid, and M. Brachet, Phys. Fluids **9**, 2644 (1997).
  - [3] M. Abid, M. Brachet, J. Maurer, C. Nore, and P. Tabeling, Eur. J. Mech. B, Fluids **17**, 665 (1998).
  - [4] T. Araki, M. Tsubota, and S. K. Nemirovskii, Phys. Rev. Lett. **89**, 145301 (2002).
  - [5] S. A. Orszag, in *Fluid Dynamics*, Proceedings of the Les Houches Summer School 1973, edited by R. Balian and J. L. Peube (Gordon and Breach, New York, 1977).
  - [6] U. Frisch, T. Matsumoto, and J. Bec, J. Stat. Phys. **113**, 761 (2003).
  - [7] C. Cichowlas and M. E. Brachet, Fluid Dyn. Res. **36**, 239 (2005).
  - [8] U. Frisch, *Turbulence, the Legacy of A. N. Kolmogorov* (Cambridge University Press, Cambridge, U.K., 1995).
  - [9] D. Gottlieb and S. A. Orszag, *Numerical Analysis of Spectral Methods* (SIAM, Philadelphia, 1977).
  - [10] G. I. Taylor and A. E. Green, Proc. R. Soc. A **158**, 499 (1937).
  - [11] M. E. Brachet, D. I. Meiron, S. A. Orszag, B. G. Nickel, R. H. Morf, and U. Frisch, J. Fluid Mech. **130**, 411 (1983).
  - [12] R. H. Kraichnan, J. Fluid Mech. **59**, 745 (1973).
  - [13] R. H. Kraichnan, Phys. Rev. **113**, 1181 (1959).
  - [14] C. Cichowlas, P. Bonaiti, F. Debbash, and M. E. Brachet (to be published).
  - [15] L. Isserlis, Biometrika **12**, 134 (1918).
  - [16] S. Dyachenko, A. C. Newell, A. Pushkarev, and V. E. Zakharov, Physica (Amsterdam) **57D**, 96 (1992).
  - [17] C. Connaughton and S. Nazarenko, Phys. Rev. Lett. **92**, 044501 (2004).
  - [18] A. J. Majda and I. Timofeyev, Proc. Natl. Acad. Sci. U.S.A. **97**, 12413 (2000).
  - [19] A. J. Majda and R. Abramov, Proc. Natl. Acad. Sci. U.S.A. **100**, 3841 (2003).